FATIGUE SURFACE CRACKS IN CAST IRON WITH NODULAR GRAPHITE

M. Schleicher*, H. Bomas*, P. Mayr*

Low cycle fatigue tests were carried out at two ductile cast irons. The growth characteristics of short surface cracks were investigated under different block loading programmes. Most cracks start at graphite nodules. The lengths of the cracks leading to failure and the crack densities were determined in dependence of the cycle number. The growth rates under short block loading are generally higher than under long block loading. It was found that the failure causing cracks consisted of up to 10 independent short cracks that had linked. The crack densities show some differences of the crack nucleation rates between the short and the long block loading condition. In general the reduced lifetime under the short block loading is caused by an interaction of higher pure growth rates and an increased propagation due to the absorption of more other cracks.

INTRODUCTION

Austempered ductile iron (ADI) is an iron with excellent mechanical properties under static load because of its exceptional combination of high strength and ductility and so it has the potential to replace forged components in order to reduce costs. So far, there has been a lack in systematic studies of ADI under cyclic loading. To understand the behaviour of ADI in the fatigue test, it is necessary to investigate the growth characteristics of short fatigue cracks, which was done in an extensive study. In general, short cracks play a dominant role in the LCF-region. Usually materials show a so called short crack effect, which means that short cracks are able to grow at levels of ΔK that are lower than the threshold value ΔK_{th} for long cracks (1, 2). Another characteristic feature of short cracks is, that they can be influenced by the microstructure of a material, grain boundaries for example. As a result of this the growth rates of short cracks often show large scatter.

* Stiftung Institut für Werkstofftechnik Bremen, Germany

RESULTS

The investigated materials were the nodular cast iron GGG-60 and the ADI version GGG-90 B, which was produced by heat treating of GGG-60 (870°C,1h → 365°C, 2h) in order to achieve a bainitic-austenitic matrix with a portion of roughly 35 % retained austenite. Table 1 shows the chemical composition, mechanical properties are given in table 2 (3).

TABLE 1 - Chemical composition, wt%

C	Si	Mn	S	Ni	Cu	Mg
3.8	2.55	0.62	0.002	0.023	0.33	0.026

Besides the determination of the nodule count per area (108 ± 17 mm^{-2}), a statistical examination of the graphite nodules diameter and the distance to the neighbouring nodule was carried out. The mean diameter of the graphite nodules is 32 ± 10 µm. 10 % of the graphite nodules have a distance < 5 µm to their neighbour. Stress controlled fatigue tests were conducted with cylindrical smooth specimens with a diameter of 8 mm in a servo-hydraulic fatigue testing machine at a frequency of 3 Hz. Constant amplitude experiments were carried out to determine the stress levels that lead to N_f = 10000 (High level) and N_f = 150000 (Low level). Both R = -1 and R = 0 stress ratios were investigated. In order to examine the influence of the load history on the number of cycles to fracture block loading experiments were carried out. Figure 1 gives an idea of the experimental programme.

Fatigue process was successively observed on the specimen surface by the aid of a plastic replication technique. It was possible to conserve the major part of the specimen surface at different numbers of load cycles. After the specimen was broken, the crack that led to failure could be traced back. In addition to that, crack densities in dependence of the cycle number were determined. Crack coalescence occurred even at low stresses and dominated the growth rates of longer cracks. It was found that the failure causing cracks consisted of up to 10 independent short cracks that had linked during the fatigue process. The majority of the cracks start from graphite nodules and microshrinkage pores, which was found by other workers too (4, 5).

TABLE 2 - Mechanical properties (3)

	$R_{p0,2}$ [MPa]	R_m [MPa]	A_5 [%]	Hardness
GGG-60	415 ± 7	733 ± 16	8 ± 2	237 ± 9 HB 2.5 30
GGG-90 B	794 ± 7	1062 ± 12	6 ± 1	350 ± 14 HV 1

Figure 2 shows the crack growth rates of the dominant cracks, that caused failure. These propagation rates display a large scatter, which is typical for short cracks. Because of

relative high surface crack densities in the investigated materials, the crack propagation rates are influenced by crack coalescence and other interactions between neighbouring cracks, causing large scatter. If the propagation rates under **HLHL1** and **HLHL2** load are compared, in spite of the scatter, in the case of **HLHL2** higher values especially for crack lengths < 200 μm can be recognized.

Table 3 shows the Miner sum D (6, 7) under block loading conditions. If the block loading conditions **HLHL1** and **HLHL2** are compared under the assumption of a linear damage accumulation rule, the values of N_f and D would remain constant. The experiment however shows that the Miner sums under the short block loading condition **(HLHL2)** are between 31 and 50 % smaller than under the long block loading condition **(HLHL1)**, which is in accordance to the behaviour of many materials. The smaller Miner sums under the short block loading condition **HLHL2** are consistent with higher crack propagation rates compared to the long block loading condition **HLHL1**.

TABLE 3 - Miner sums D in the block loading tests

	D(HLHL1)		D(HLHL2)	
Material	R = -1	R = 0	R = -1	R = 0
GGG-60	0.62 ± 0.09	1.04 ± 0.14	0.42 ± 0.09	0.63 ± 0.04
GGG-90 B	1.44 ± 0.29	1.61 ± 0.13	0.72 ± 0.11	1.13 ± 0.09

So the smaller Miner sums under **HLHL2** can be explained with higher crack propagation rates. One reason could be different crack densities under the loading conditions **HLHL1** and **HLHL2**. It is well known that the crack density has an influence on the propagation rate (8). In general, one can separate pure growth and propagation due to the absorption of other cracks located in the growth plane of the dominant crack. It is obvious that a higher crack density leads to a higher propagation rate due to crack coalescence. Extensive investigations of the crack densities in dependence of the number of load cycles show some references to differences of the crack nucleation rates between the loading conditions **HLHL1** and **HLHL2** but only at GGG-60 R = 0 and GGG-90 B R = -1 the crack densities at a certain number of load cycles are significant higher.

Differences in the pure crack growth rates of long cracks in steel and aluminium alloys were often investigated. A change of the stress amplitude from low to high leads to an accelerated growth rate, whereas a change from high to low leads to a retarded growth rate. Often these effects are explained with differences in the crack closure behaviour (9, 10, 11). Results of crack closure measurements of short fatigue cracks in ferritic-pearlitic and austempered ductile iron could not be found in the literature.

SUMMARY

The block length has a strong influence on the lifetime in the fatigue test of specimens made of ductile cast irons. A reduced block length leads to a decreasing number of cycles to failure. There is a close connection between the growth behaviour of short cracks and the number of cycles to failure. The propagation rates of the failure causing cracks under short block loading are higher than under long block loading. It was found that the failure causing cracks consisted of up to 10 independent short cracks that had linked. Because of this the crack densities were investigated. There are some differences of the crack nucleation rates between the short and the long block loading condition. In general the reduced lifetime under the short block loading is caused by an interaction of higher pure growth rates and an increased propagation due to the absorption of more other cracks. Further work will be necessary to clarify the observed effects of acceleration and retardation on the crack propagation rates.

Symbols Used

A_5	= fracture elongation
K	= stress intensity factor
ΔK	= stress intensity factor range
ΔK_{th}	= threshold of stress intensity factor range for long crack growth
a	= crack depth
2c	= surface crack length
D	= Miner sum
dc/dN	= velocity of surface cracks
H	= constant amplitude loading with high stress amplitude
L	= constant amplitude loading with low stress amplitude
HL	= loading sequence high-low
LH	= loading sequence low-high
HLHL1	= block programme with long block lengths
HLHL2	= block programme with short block lengths
N_f	= number of cycles to failure
R	= ratio of minimum and maximum stresses
R_m	= ultimate tensile strength
$R_{p0.2}$	= yield strength
σ_a	= stress amplitude

ACKNOWLEDGEMENTS

This work was funded by the „Arbeitsgemeinschaft industrieller Forschungsvereinigungen (AiF)“ and the Bundesministerium für Wirtschaft (AiF-number 9673B).

REFERENCES

(1) Miller, K. J., Materials Science and Technology, Vol. 9, 1993, pp. 453-462

(2) Schijve, J., "Predictions on fatigue life and crack growth as an engineering problem. A state of the art survey" Proceedings of the sixth international fatigue congress "Fatigue '96". Edited by Lütjering, G. and Nowack, H., Berlin, 1996, pp. 1149-1164

(3) Böschen, R., "Schwingfestigkeitsverhalten von randschichtgehärtetem bainitisch-austenitischen Gußeisen mit Kugelgraphit", VDI-Fortschrittbericht Reihe 18 Nr.168, Düsseldorf, 1985

(4) Lin, C.-K. and Lai, P.-K.; Shih, T.-S., Int. J. Fatigue, Vol. 18, 1996, pp. 297-307

(5) Lin, C.-K. and Hung, T.-P., Int. J. Fatigue Vol. 18, 1996, pp. 309-320

(6) Palmgren, A., VDI-Zeitschrift, Vol. 68, 1924, pp. 339- 341

(7) Miner, M. A., Trans. ASME, J. Appl. Mechanics, Vol. 12, 1945, pp. A159-A164

(8) Bomas, H., Linkewitz, T. and Mayr, P., Fatigue Fract. Eng. Mater. Struct., Vol. 19, 1996, pp. 299-307

(9) Buschermöhle, H., Vormwald, M. and Memhard, D., "Einfluß von Überlasten auf die Rißfortschrittslebensdauer", DVM-Bericht 800, 1997, pp. 93-115

(10) Davidson, D. L., "The experimental mechanics of microcracks", in: "Small-Crack Test Methods", ASTM STP 1149. Edited by Larsen, J. M. and Allison, J. E., Philadelphia, 1992, pp. 81-91

(11) Dabayeh, A. A. and Topper, T. H., Int. J. Fatigue, Vol. 17, 1995, pp. 261-269

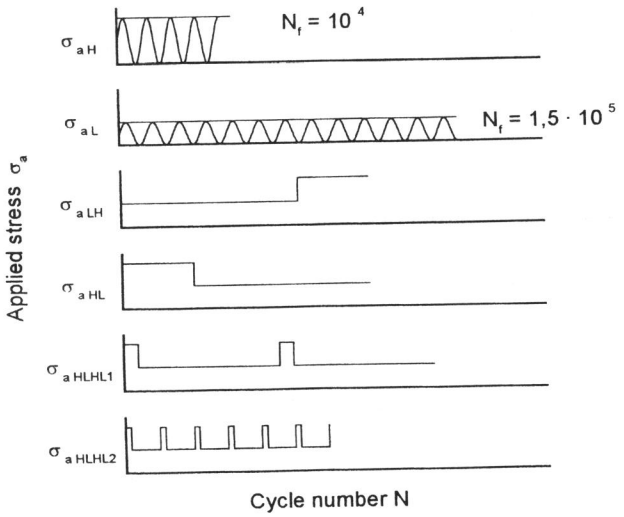

Figure 1 Schematic sketch of the experimental programme

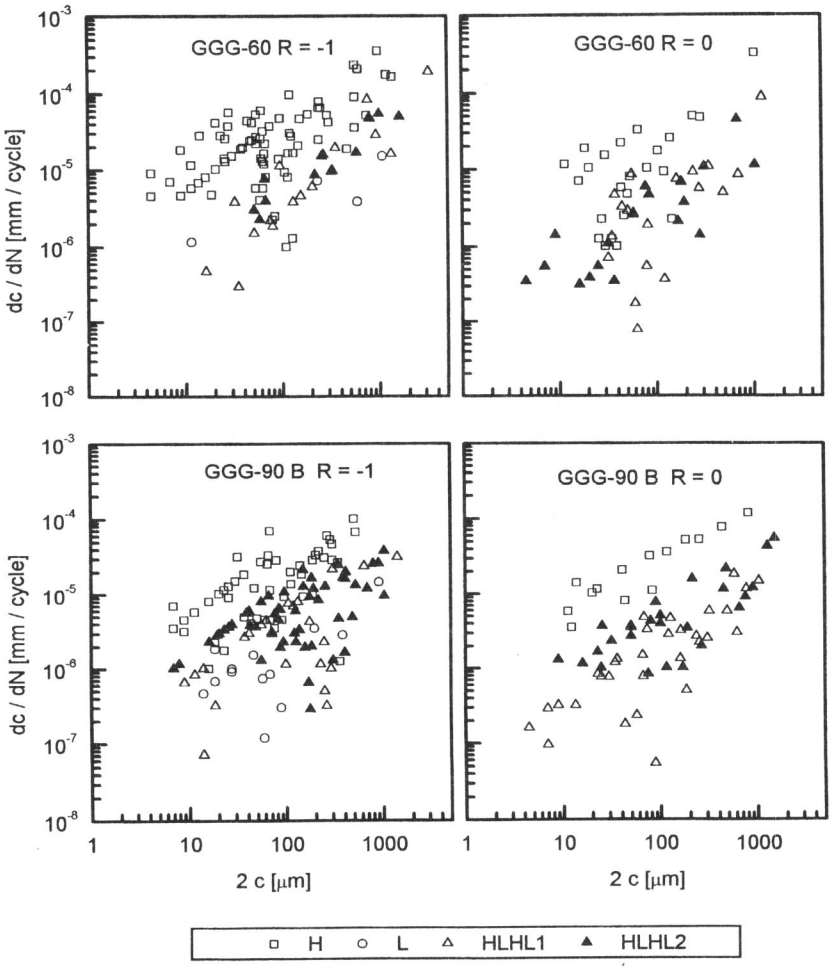

Figure 2 Surface propagation rates of cracks leading to failure under different load conditions